FIZIKA, 7 (1975) 71—82

ATTENUATION OF ELECTRON WAVES ON DRIFTING PLASMAS

B. A. ANIČIN and V. M. BABOVIĆ

Institute of nuclear sciences »Boris Kidrič«, Beograd

Received 14 February 1975

Abstract: Measurements of electron waves attenuation on drifting plasmas are described. The results are given for mercury pool temperatures of 10°, 15° and 20°C. From the theoretical point of view various physical mechanisms leading to damping are described: collisional loss due to electron-atom collisions, collisionless Landau damping and dielectric loss in the discharge tube walls. The total attenuation coefficient is derived as a sum of the various contributing effects. Comparison of theory and experimental data is presented.

1. *Introduction*

It was first predicted theoretically by Trivelpiece and Gould[1] that an electron wave travelling on a column of drifting plasma should have different wavenumbers and group velocities in the upstream and downstream direction, due to the Doppler effect introduced by the plasma drift velocity. Although the prediction was made at a fairly early stage of plasma electron wave studies, very little use was made of it in practical plasma diagnostics. One of the causes of the scarcity of observation of differences in upstream-downstream wave properties is possibly related to the fact that most authors [2,3] have conducted standing wave measurements which invariably yield unresolved arithmetic means of upstream and downstream wavenumbers and attenuation coefficients.

Observations of differences in upstream and downstream propagation of electron waves on positive columns have been reported previously by the authors[4].

The experimental data can be grouped around three basic effects caused by the electron drift velocity:

- differences in the real part of the wave-number,
- differences in the imaginary part of the wavenumber i. e. attenuation effects, and
- differences in initial wave amplitudes.

The interpretation of phenomena related to the real part of the wavenumber has led to a verification of the Lorentz dragging coefficient in dispersive media, and is described elsewhere[5]. Differences in initial wave amplitudes can be put to the useful purpose of determining electron drift velocities, and the authors hope to be able to report on this shortly.

The aim of this paper is to describe measurements of wave damping in a drifting bounded plasma and correlate attenuation data with theory i. e. to deal with second point above.

2. *Experiments*

The apparatus has been described extensively in the paper[6], therefore only a brief description of the method will be given (Fig. 1). In one set of experiments the wave launcher was kept in the middle of the usable length of the discharge tube positive column (approx. 700 mm) and operated CW at 125 and 250 MHz. Waves were launched towards the cathode, at the left end of the tube, and towards the anode at the right end of tube. A wire probe connected to a sampling oscilloscope was used to detect the wave at fixed sampling time, which permitted to plot the wave field $E(z, t)$ for $t = \text{const.}$ directly on a chart recorder and almost simultaneously for both directions. Some of the results are shown in Fig. 2, from which three conclusions can be drawn:

- downstream wavenumbers (k_r^+) are smaller than upstream wavenumbers (k_r^-)
- the downstream wave is less attenuated than the upstream wave, and
- the downstream wave amplitude is larger than the upstream amplitude.

The last property is unconnected with wave attenauation, as the two amplitudes differ in the immediate vicinity of the launcher.

Several pitfalls have to be carefully avoided to obtain valid attenuation data on drifting plasmas. One of these has its origin in low-frequency fluctuations in the tube, and is known as phase scrambling or phase jitter[7]. Although the degree of turbulence (relative fluctuations in electron density) is low, between 0.5 and 2%, and of the same order as in plasmas conventionally described as quiescent, the effect can be clearly seen on the sampling oscilloscope screen[8] and tends to

produce too large attenuation coefficients as the level of low frequency fluctuations is increased. The chart recorder output of the sampling oscilloscope tends to average out the fluctuating waveform, and produces apparent wave damping much in the same fashion as in interferometer devices or narrow band receivers.

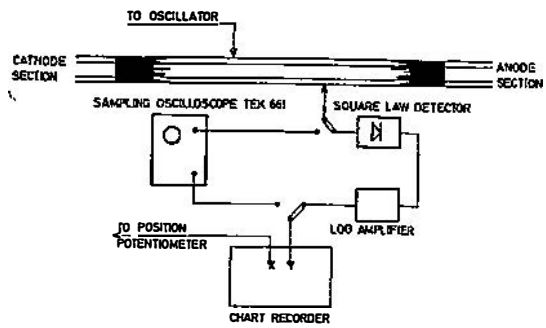

Fig. 1 Experimental setup.

To avoid phase scrambling effects, we have used the sampling oscilloscope only for the determination of the real part of the wavenumber, whereas all attenuation measurements have been conducted with a simple square law detector followed by a logarithmic amplifier. This method is free of phase jitter effects on principle, as the change in phase cannot affect the output of a square law diode. It has the disadvantage that the law of the detector has to be exactly known within the operating signal level range. The detector law was established by comparison with the sampling oscilloscope which is a linear device and by monitoring the

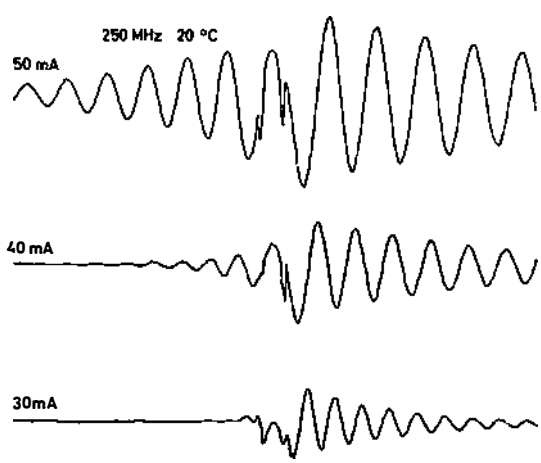

Fig. 2. Chart recorder traces of sampling oscilloscope output at three arc currents.

oscillator output with a calibrated V. H. F. voltmeter. Both methods give $g = 1.95$ for the exponent in the detector law. The method was proved to be fluctuation independent, by deliberate low-frequency modulation of arc current up to 5% and by deliberately increasing stochastic fluctuations in electron density with a permanent magnet in the cathode section of the tube. Some of the diagrams obtained by this method are shown in Fig. 3, where the slope is directly proportional to the imaginary part of the wavenumber or attenuation coefficient. In fact, all final measurements were conducted with the launcher at one end of the tube, to increase accuracy. Fig. 3 illustrates the difference in upstream and downstream wave damping, which in fact is of such magnitude that the device could be easily used as an electrically controlled non-reciprocal isolator based on electron drift, if not for the noise and general unreliability associated with all gaseous plasma devices.

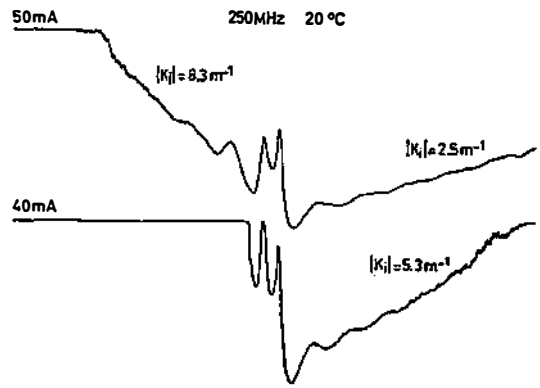

Fig. 3. Chart recorder traces of the square-law detector followed by the logarithmic amplifier. The slope is directly proportional to $|k_i|$.

It was found essential to terminate both the cathode and anode end of the tube with carefully designed aquadag terminations, and a lot of experimentation went into the reduction of the reflection coefficients of these absorbers. The fact that nonreflecting terminations are required in the measurement of wave properties on drifting plasmas can be easily understood on theoretical grounds[4] and explains why the left-right unsymmetry was not noticed in previous experiments[2].

The real and imaginary parts of the wavenumber were measured at different mercury vapour pressures in the tube (0.064 Pa, 0.104 Pa, 0.163 Pa and 0.248 Pa, corresponding to mercury pool temperatures of 10, 15, 20 and 25°C.). Data are presented in Section 4.

3. Theory

The great complexity of phenomena leading to wave damping in bounded, inhomogeneous and drifting plasmas excludes the direct application of a single theory to interpret the experimental data. We analize the various physical mechanisms leading to damping, such as collisional loss due to electron-atom collisions, collisionless Landau damping and dielectric loss in the discharge tube walls, and derive total attenuation coefficients as a sum of the various contributing effects.

Collisional damping. Although this is the simplest type of loss, some care must be excercised to take drift into account. We consider a homogeneous plasma, and depart from the Boltzmann equation

$$\frac{\partial \vec{v}}{\partial t} + (\vec{u}\,\nabla)\vec{v} = -\frac{e}{m}\vec{E} - \frac{e}{m}\vec{u} \times \vec{B} - \nu\,\vec{v}, \tag{1}$$

and the continuity equation

$$\frac{\partial n}{\partial t} + \operatorname{div}(n_0 \vec{v}) + \operatorname{div}(n\vec{u}) = 0, \tag{2}$$

where ν is the effective collision frequency for momentum transfer. The wave quantities are written as $\exp(i(kz - \omega t))$, where z is the direction of wave propagation. Using Maxwell's equations and applying boundary conditions with due care because of the drift velocity, we arrive at the imaginary part of the impedance of the plasma cylinder and obtain wave damping by a perturbation technique in the form

$$k_i^{\nu} a = \frac{A\,a_5 \dfrac{1 - \bar{\varepsilon}_p}{\bar{\varepsilon}_p} \dfrac{\nu}{\bar{\omega}}}{\dfrac{\partial}{\partial A}\left\{A\,a_5\left[1 - \dfrac{\bar{\varepsilon}_p}{\varepsilon_r}\dfrac{R - a_6}{R + a_7}\right]\right\}}, \tag{3}$$

where $\bar{\omega} = \omega - k\,u$ is the Doppler shifted frequency, $\bar{\varepsilon}_p = 1 - \omega_p^2/\bar{\omega}^2$ and the various ratios of Bessel functions are denoted by

$$\begin{aligned}
a_1 &= \frac{K_0(B)}{K_1(B)}, & a_2 &= \frac{I_0(B)}{I_1(B)}, \\
a_3 &= \frac{K_0(B)}{I_0(B)}, & a_4 &= \frac{K_1(B)}{I_1(B)}, \\
a_5 &= \frac{I_0(A)}{I_1(A)}, & a_6 &= \frac{K_0(A)}{I_0(A)}, \\
a_7 &= \frac{K_1(A)}{I_1(A)},
\end{aligned} \tag{4}$$

with $A = k_r a$ and $B = k_r b$ and

$$R = \frac{a_3 - \varepsilon_r a_1 a_4/a_5}{1 + \varepsilon_r a_1/a_2}. \tag{5}$$

The collision frequencies ν in the pressure range of interest can be found in the literature[9]. The results of the computation for 20°C are shown in Fig. 4. Similar curves are obtained for other pressures.

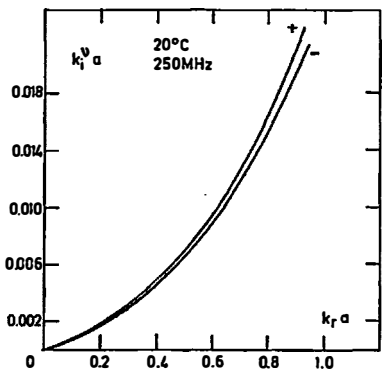

Fig. 4. Theoretical results for collisional damping. Frequency 250 MHz, mercury pool temperature 20°C, collision frequency for momentum transfer $19 \cdot 10^6\ s^{-1}$.

This perturbation technique was first applied in[1]. The procedure is correct provided the ratio of collision frequency and wave angular frequency $\frac{\nu}{\omega}$ is small compared to unity, which is safely satisfied in our case as $\frac{\nu}{\omega}$ does not exceed 0.01.

Collisionless effects. Landau damping. Landau was the first to show[10] the existence of a collisionless mechanism of wave damping in an infinite plasma. For a semi-space of plasma an analogous solution is given by Romanov[11]. Kondratenko has developed solutions for a planar plasma slab and a cylindrical plasma[12,13]. With the necessary generalization to take into account drift velocity, we follow here the procedure outlined in[13]. We start with the collisionless Boltzmann equation

$$\frac{\partial F}{\partial t} + \vec{v}\frac{\partial F}{\partial \vec{r}} + \frac{e}{m}(\vec{E} + \vec{v} \times \vec{B})\frac{\partial F}{\partial \vec{v}} = 0, \tag{6}$$

and consider an axially symmetric mode with field components E_r, E_z, H_φ, as before. For the zero order distribution function f_0 we take a shifted Maxwellian

$$f_0 = \frac{n_0}{\pi w^2} e^{-\frac{v_r^2 + v^2}{w^2}}, \tag{7}$$

where n_0, the electron density in the positive column, is constant by assumption, $w = (2 \varkappa_B T/m)^{1/2}$ is the most probable speed in the Maxwell distribution, $V = v_z - u$, and v_r and v_z are the radial and axial velocity components, respectively. Introducing the perturbation part of the distribution function, we have

$$F = f_0 + f \tag{8}$$

and after linearization

$$\frac{\partial f}{\partial r} - i\gamma f + e f_0' \left\{ E_r + \frac{V}{v_r} E_z - \mu_0 u H_\varphi \right\} = 0, \tag{9}$$

with $\gamma = (\omega - k v_z)/v_r$ and f_0' is the derivative with respect to energy, and μ_0 stands as the conventional notation for the permeability of free space. Instead of f it is useful to introduce f^+ and f^-, distribution functions defined by $f^+ = f(v_r > 0)$ and $f^- = f(v_r < 0)$, and denote

$$\begin{aligned} \psi^+ &= f^+ + f^-, \\ \psi^- &= f^+ - f^-, \end{aligned} \tag{10}$$

so that two equations containing the functions ψ^+ and ψ^- can be formed instead of Equ. (9). These equations are solved by developing the radial component of the electric field in a Fourier-Bessel series

$$E_r(r) = \frac{2}{a^2} \sum_{n=1}^{\infty} E_r^n \frac{J_0\left(j_{1n} \frac{r}{a}\right)}{J_1'^2(j_{1n})}, \tag{11}$$

The azimuthal component of the magnetic field $H_\varphi(r)$ and the function $\psi^-(r)$ are developed in series of the same type. The axial component of the electric field is developed in a Dini series

$$E_z^n(r) = \frac{2}{a^2} \sum_{n=1}^{\infty} E_r^n \frac{J_1\left(j_{1n} \frac{r}{a}\right)}{J_1'^2(j_{1n})} \tag{12}$$

as well as the function $\psi^+(r)$. We assume that the reflection of electrons from the wall is specular which entails $f^+(a) = f^-(a)$, a condition we secure by letting $\psi^-(a) = 0$. E_r^n, E_z^n, etc. are constants in the respective series. We have denoted by j_{1n} the n^{th} zero of the first order Bessel function $J_1(x)$.

The distribution functions ψ^+ and ψ^- are determined by this procedure, which makes possible the computation of radial and axial current densities j_r and j_z and therefore the use of Maxwell's equations. Applying carefully boundary conditions to a current carrying plasma[14], we arrive at a characteristic equation where an imaginary part, small by assumption, stems from collisionless Landau

damping. The imaginary part of the wavenumber is then obtained from the complex dispersion relation by a perturbation method

$$k_i^L a = 2\sqrt{\pi}\,\varepsilon_r \frac{\dfrac{1-\varepsilon_3}{\varepsilon_3}\left(\dfrac{\varepsilon_3}{\varepsilon_1}\right)^2\left\{1+2\dfrac{\omega}{\bar{\omega}}\dfrac{\bar{\omega}^2}{w^2 k^2}\left[1+\dfrac{\bar{\omega}^2 k_0^2 \varepsilon_1}{\omega^2 k^2}\right]\right\}\Sigma \dfrac{x_n \exp(-x_n^2)}{\{j_{1n}^2 + A^2 \varepsilon_3/\varepsilon_1\}^2}}{\dfrac{\partial}{\partial A}\left\{A\left[\dfrac{\varepsilon_r}{\varepsilon_1}\dfrac{I_0(A\sqrt{\varepsilon_3/\varepsilon_1})}{\sqrt{\dfrac{\varepsilon_1}{\varepsilon_3}}\,I_1(A\sqrt{\varepsilon_3/\varepsilon_1})} - \alpha_5\dfrac{R-\alpha_6}{R+\alpha_7}\right]\right\}}, \tag{13}$$

where, together with previously defined quantities, we have I_0 and I_1 as modified Bessel functions, $\varepsilon_1 = 1 - \omega_p^2/\bar{\omega}^2$, $\varepsilon_3 = 1 - \omega_p^2/(\omega\bar{\omega})$, $k_0^2 = \omega^2 \mu_0 \varepsilon_0$ is the square of the space wavenumber. The summing runs over the zeroes j_{1n} in the expression

$$x_n = \frac{\bar{\omega}\, a}{j_{1n}\, w}. \tag{14}$$

Results of computation for a pressure of 0.104 Pa and corresponding electron temperature of $5.5 \cdot 10^4$ K are shown in Fig. 5 in the experimentally relevant range of $k_r a$. Let us remark that the theory of Landau damping must be adapted to the bounded case as done above; the infinite plasma theory yields incomparably lower values of attenuation coefficients, and the effects imposed by the presence of a boundary are thoroughly discussed in the references mentioned previously.

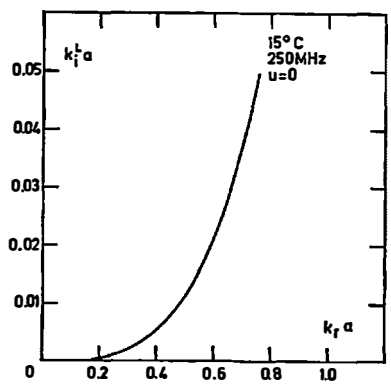

Fig. 5. Landau damping in a stationary plasma. Frequency 250 MHz, mercury pool temperature 20°C

Collisionless effects. Resonant absorption. Apart from Landau damping, associated with acceleration of a group of electrons synchronous with the wave, an almost collisionless effect is connected with resonant absorption of energy in a layer of plasma where the cold plasma dielectric vanishes. To take this effect into

account we have generalized the theory developed by Stepanov[15] by introducing drift terms. The analysis of data obtained has led to two conclusions:

– the gradient of electron density in the resonant layer is too low and the correct linear theory of the phenomenon should keep both higher order derivatives of electron density and finite collision frequency; the passage to the limit $\nu \to 0$ is not valid with the particular density profile in our plasma,

– although we know from experiment that the overall phenomenon is linear, we cannot guarantee that the conditions for valid resonant absorption[16] are satisfied, as the local field in a region of very low density can exceed the bounds for linear oscillations without impairing overall linearity.

As both a sufficiently high value of the electron density gradient and a sufficiently low value of the electric field in the resonant region are essential to the linear theory of resonant absorption, we have refrained from comparing this theory with experiment.

Dielectric loss in the glass of the discharge tube. We consider a cylindrical plasma bound by a glass tube of inner radius a and outer radius b. The real part of the glass dielectric constant is denoted by ε_r and loss is characterized by the loss tangent $\operatorname{tg}\delta$. Solving Maxwell's equations for this configuration leads to a characteristic equation which in general depends on the glass dielectric constant

$$F(\varepsilon) = 0. \tag{15}$$

Assuming moderate loss, ε_i, the imaginary part of ε is small with respect to ε_r, and the function F can be developed in a series where only the first linear terms are relevant, which leads to the final expression for dielectric loss in the glass

$$k_i' a = \frac{\varepsilon_r \operatorname{tg}\delta}{v_g} \frac{\partial Y}{\partial \varepsilon_r}. \tag{16}$$

Here k_i' is the imaginary part of the wavenumber, $Y = \dfrac{\omega}{\omega_p}$ is the ratio of signal and plasma frequency, $A = k_r a$ is the normalized real part of the wavenumber and $v_g = \dfrac{\partial Y}{\partial A}$ is the normalized group velocity. The diferentiation appearing in Equ. (16) are carried out numerically, using the characteristic equation of a current carrying cold homogeneous plasma. A sample of computation is shown in Fig. 6. The $\pm$ sign corresponds to downstream and upstream propagation, respectively. The drift velocity is $4.6 \cdot 10^7 \dfrac{\text{cm}}{\text{s}}$, corresponding to a mercury vapour pressure of 0.163 Pa. All other values are selected to match the data of our experiment: $\varepsilon_r = 4.8$, $\operatorname{tg}\delta = 0.014$, $a = 0.6$ cm, $b = 0.77$ cm. Similar results are obtained for

other pressures. Setting the drift velocity of the electrons equal to zero, $u = 0$, yields results already obtained in[17], where this perturbation procedure was originally described.

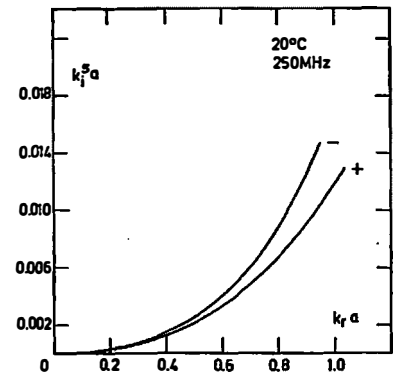

Fig. 6. Dielectric loss in the tube glass. Frequency 250 MHz, mercury pool temperature 20°C loss tangent $1.4 \cdot 10^{-2}$.

4. *Comparison of theoretical and experimental results — conclusions*

Comparison of theory and experimental data is presented in Figs. 7—12. The solid lines in these diagrams refer to total damping computed from equations (3), (13) and (16) representing collisional loss, Landau damping and dielectric loss in the glass. Damping due to resonant absorption is not included, as the conditions of applicability of the linear version of this theory are not satisfied in our experiment.

All computations presented in the figures have been done for an operating frequency of 250 MHz. Landau damping is generally the more important factor

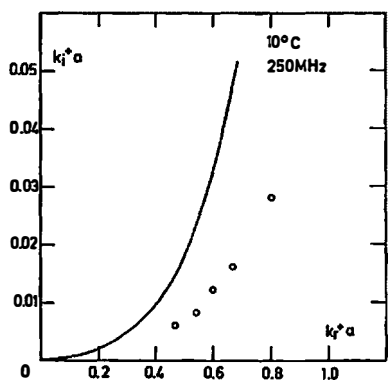

Fig. 7. Comparison of experiment and theory (250 MHz, 10°C, downstream propagation).

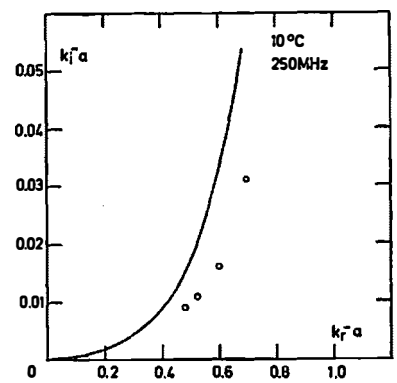

Fig. 8. Comparison of experimet and theory (250 MHz, 10°C, upstream propagation).

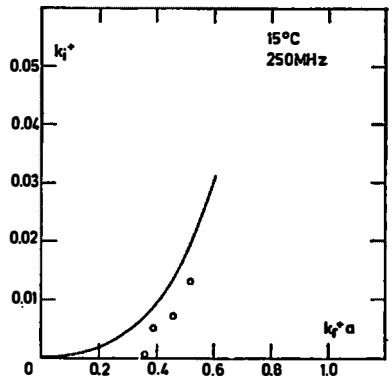

Fig. 9. Comparison of experiment and theory (250 MHz, 20°C, downstream propagation).

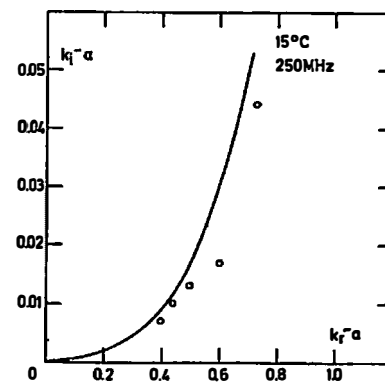

Fig. 10. Comparison of experiment and theory (250 MHz, 20°C, upstream propagation).

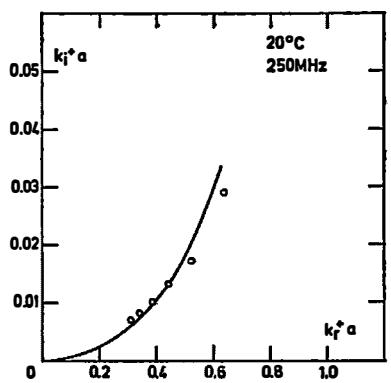

Fig. 11. Comparison of experiment and theory (250 MHz, 20°C, downstream propagation).

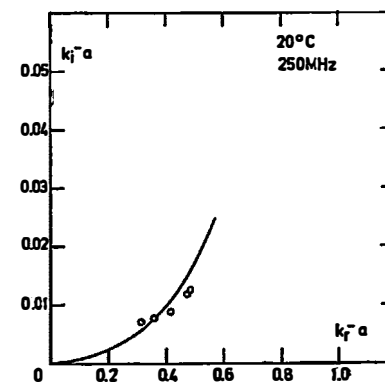

Fig. 12. Comparison of experiment and theory (250 MHz, 20°C, upstream propagation).

than collisional loss, and collisional loss is generally larger or comparable to the dielectric loss in the glass. Agreement between results of theory and experiment is very good at mercury pool temperature of 20°C, corresponding to a mercury vapour pressure of 0.163 Pa, and worsens as the mercury pool temperature is lowered.

References

1) A. W. Trivelpiece and R. W. Gould, Journ. Appl. Phys., **30** (1959) 1784;
2) D. B. Ilić and B. A. Aničin, Int. J. Electronics, **28** (1970) 41;
3) Y. Ida and K. Hayashi, Journ. Appl. Phys., **42** (1970) 2423;
4) B. A. Aničin, V. M. Babović and D. M. Šulić, Proc. 11th Int. Conf. on Phen. in Ion. Gases, Prague, (1973) p. 357;

5) B. Aničin and V. Babović, Proc. 7th Yugoslav Symposium on Physics of Ionized Gases, Rovinj (1974) p. 185;
6) B. A. Aničin, V. M. Babović and K. E. Lonngren, I. Plasma Physics, **7** (1972) 403;
7) B. A. Aničin and D. B. Ilić, Journ. Appl. Phys., **41** (1970) 2737;
8) B. A. Aničin, Proc. Int. Summer School on the Physics of Ionized Gases, Hercegnovi, Yugoslavia, (1970) p. 586;
9) V.E. Golant, High-frequency methods of plasma investigation (in Russian), Nauka, Moscow, (1968) p. 15;
10) L. D. Landau, ZhETF, **16** (1946) 574;
11) Y. A. Romanov, Radiofizika, **7** (1964) 242;
12) A. N. Kondratenko, Nuclear Fusion, **5** (1965) 267;
13) A. N. Kondratenko, ZhTF, **42** (1972) 743;
14) A. B. Mihailovski and E. A. Pashitski, ZhETF, **48** (1965) 1787;
15) K. N. Stepanov, ZhTF., **35** (1965) 1002;
16) B. A. Aničin, Proc. 5th European Conference on Controlled Fusion and Plasma Physics, Grenoble, (1972) p. 119;
17) B. A. Aničin, Fizika, **1** (1968) 69.

SLABLJENJE ELEKTRONSKIH TALASA NA POKRETNIM PLAZMAMA

B. A. ANIČIN i V. M. BABOVIĆ

Institut za nuklearne nauke »Boris Kidrič«, Beograd

Sadržaj

Opisana su merenja slabljenja elektronskog talasa na pokretnoj ograničenoj plazmi. Priloženi su rezultati za temperature živinog rezervoara 10, 15 i 20°C. Teorijske vrednosti za slabljenje računate su zbrajenjem tri nezavisna faktora: kolizionog slabljenja, Landauovog slabljenja i slabljenja zbog gubitaka u staklu. Razmatrano je i pitanje rezonantne apsorpcije. Eksperimentalni i teorijski rezultati su upoređeni.